

# Use of Long-Range C-H ( ${}^nJ_{CH} n>3$ ) Heteronuclear Multiple Bond Connectivity in the Assignment of the ${}^{13}\text{C}$ NMR Spectra of Complex Organic Molecules

Ramiro Araya-Maturana,\*<sup>1</sup> Tomás Delgado-Castro,<sup>1</sup> Wilson Cardona<sup>1</sup> and Boris E. Weiss-López<sup>2</sup>

1. Departamento de Química Orgánica y Físicoquímica, Facultad de Ciencias Químicas y Farmacéuticas, Universidad de Chile, Casilla 233, Santiago 1, Chile

2. Departamento de Química, Facultad de Ciencias, Universidad de Chile, Casilla 653, Santiago, Chile

**Abstract :** The structural elucidation of complex organic molecules relies heavily on the application of proton detected heteronuclear NMR. Among these techniques, the HMBC NMR experiment is probably the most useful 2D NMR method. The HMBC (C-H) experiment allows the assignment of structural fragments through correlations between protons and carbons separated by more than one bond, usually two or three bonds ( ${}^2J_{CH}$  and  ${}^3J_{CH}$ ) via  ${}^1\text{H}$ ,  ${}^{13}\text{C}$ -coupling constants. It is also possible to obtain valuable information through longer correlations,  ${}^nJ_{CH} n>3$ , performing several HMBC experiments with different long-range delays and using a deeper threshold in the contour plot. There have been several attempts to improve the results of the HMBC experiment, mainly focused on the question of optimization of the long-range delay, <sup>2</sup>. The D-HMBC, 3D-HMBC, CT-HMBC, ACCORD-HMBC, IMPEACH-MBC and CIGAR-HMBC experiments which provide much better experimental access to sample long-range couplings are briefly discussed. These long-range correlations have proven to be crucial in the structure elucidation of molecules with proton deficient skeleton.

## INTRODUCTION

In this review we will focus our attention only on Heteronuclear Multiple Bond Correlation (HMBC) [1-3] and modifications of it. Other types of heteronuclear correlation experiments will not be treated here, since HMBC is the most widely used experiment to observe  ${}^{13}\text{C}$ - ${}^1\text{H}$  long range couplings.

The structural elucidation of complex organic molecules relies heavily on the application of proton detected heteronuclear NMR. Among these techniques, the HMBC NMR experiment is probably the most useful 2D NMR method [4], since it detects  ${}^{13}\text{C}$ - ${}^1\text{H}$  long range couplings using inverse detection of the  ${}^1\text{H}$  signal, the most sensitive NMR nucleus. Inverse detection techniques also present a considerably higher sensitivity when compared to older 2D experiments [5]. The sensitivity is particularly good when the  ${}^1\text{H}$  signals to be observed appear as sharp lines. The HMBC experiment gives a wealth of structural and assignment information through long-range correlation signals for C,H spin pairs, that can span quaternary carbons or heteronuclei, providing a way to link structural fragments together. Therefore, it can be efficiently used to elucidate the molecular skeleton. Two reviews on this topic were published about ten years ago [5,6]. The use of HMBC in

concert with Heteronuclear Multiple Quantum Coherence, HMQC [7], has proven to be extremely useful for the total structure elucidation and NMR spectral assignments of numerous natural products and complex organic molecules. At the beginning, the sensitivity of HMBC was low as compared with HMQC; however, this characteristic has improved significantly with the introduction of pulsed field gradients [8-10] into these experiments in the early 1990's. It allowed the receiver gain of the spectrometer to be significantly raised, since the unwanted coherences were already filtered off in the probe head. Moreover, the addition of pulsed field gradients into NMR pulse sequences yields spectra with fewer artifacts and decreases the data collection time, because the selection of the desired coherence pathways occurs without extensive phase cycling. Today, the gradient modification of the HMBC sequence [11] has become a routine standard, accessible to most operators of NMR instruments capable to generate pulsed gradients.

Generally, the HMBC (C-H) experiment is described as a technique that allows the assignment of structural fragments through correlations between protons and carbons that are separated by more than one bond, usually through two or three bonds ( ${}^2J_{CH}$  and  ${}^3J_{CH}$ ) [11,12] via  ${}^1\text{H}$ ,  ${}^{13}\text{C}$ -coupling constants, despite the early observation of a crucial four bond C-H correlation in the HMBC spectrum of antibiotic distamycin A [5]. The valuable information that can be obtained through these correlations ( ${}^nJ_{CH} n>3$ ), is generally discarded because the relative intensities of the resonances are directly related to the magnitude of the coupling constants. Therefore, for  ${}^nJ_{CH} n>3$  the cross peaks show a low intensities. This characteristic has been used as a criterion to

\*Address correspondence to this author at the Departamento de Química Orgánica y Físicoquímica, Facultad de Ciencias Químicas y Farmacéuticas, Universidad de Chile, Casilla 233, Santiago 1, Chile; Tel.: +56-2-6782865; Fax: +56-2-6782868; e-mail: raraya@ciq.uchile.cl

discard signals in a computational method of analysis of 2D NMR spectra [13].

## EXPERIMENTAL DETAILS

When the signals appear as broad lines due to complex splittings, HMBC suffers from a considerable lack of sensitivity. As a consequence, the detection of cross peaks becomes difficult. This problem arises when the power mode data processing causes the cancellation of antiphase signal components. The situation is made worse when the separation of these components is small and when their signals are broad. The efficiency of the HMBC technique is affected also by spectrometer instabilities resulting in  $t_1$ -noises ridges, which also originate from protons bound to  $^{12}\text{C}$ . This problem is solved by the application of pulsed field gradients [8-10] leading to much better results in a fraction of the time, since the unwanted coherences are already filtered off in the probe head.

A second problem associated with inverse proton-detected heteronuclear shift correlation experiments is the lack of resolution in the indirectly detected dimension ( $F_1$ ). For a given spectral width, an increase in  $F_1$  resolution requires an increase in the number of  $t_1$  increments. Generally, not all spectral regions are crowded enough to need such a treatment.  $F_1$  restricted 2D maps can be a great help to ensure a proper spectral analysis [14].

Theoretically, in the HMBC pulse sequence the optimum choice for the first delay is calculated from the expression  $\tau_1 = 1/(2 \ ^1J(\text{C,H}))$ . Generally, the  $^1J(\text{C,H})$  coupling constants span a range of values from 130 to 160 Hz. The  $^1J(\text{C,H})$  filter delay in the pulse sequence currently implemented, is calculated by entering an average value of  $^1J_{\text{CH}}$ , usually 140 or 125 Hz, depending on whether there are aromatic or alkene groups, respectively, giving a value of  $\tau_1 = 3.6$  or 4.0 ms. In the same manner, the optimum value of the second delay is calculated from  $\tau_2 = 1/(2 \ ^nJ(\text{C,H}))$ , where  $^nJ(\text{C,H})$  is the long range coupling constant. However a drawback of the experiment is due to the range of values of  $^2J(\text{C,H})$  and  $^3J(\text{C,H})$  spin coupling constants, which can

have values from 1 to 25 Hz. In practice, a delay shorter than the theoretical value, 65 to 100 ms, is employed to avoid the decay of the  $^1\text{H}$  magnetization during this delay [15]. Usually, the experimental settings of these parameters in the HMBC experiment are the result of a compromise: when the spin coupling constant is about 8 Hz, the  $\tau_2$  delay in the sequence is about 60 ms, allowing an optimum transfer for correlations.

The pulse sequence of the HMBC experiment is shown in Fig. (1) [11].

Running the experiment under these conditions, several important couplings could give rise to only very small correlation signals, or they may be completely lost.

Furthermore, the direct translation of the connectivities observed in the HMBC spectrum into the bonding network, may be hampered by the fact that  $^2J_{\text{CH}}$  and  $^3J$  correlations cannot be distinguished [13].

Different methods have been developed to solve both problems mentioned before. In particular, a method to distinguish between  $^2J_{\text{CH}}$  and  $^3J_{\text{CH}}$  correlations obtained in HMBC experiments has been described some years ago. The experiment is known as 1,1-ADEQUATE and yields only two bond  $^1\text{H}$ - $^{13}\text{C}$  connectivities in H-C-C moieties, allowing differentiation of HMBC from two and three  $^1\text{H}$ - $^{13}\text{C}$  bond connectivities [12, 15]. An additional advantage of this method is that it permits to observe correlations that are missing in the HMBC experiment.

In general, the observed correlations in different HMBC experiments depend on the value the long-range delay, obtained from the individual long-range C-H coupling constant responsible for creating the heteronuclear multiple quantum coherence. Usually, the long-range delay is optimized for a value between 5 and 10 Hz for  $^1\text{H}$ - $^{13}\text{C}$  long-range correlation experiments. The choice is generally made on an arbitrary basis rather than from a knowledge of the actual value of the couplings. On this basis, a first approximation to observe more long-range correlations is to perform several HMBC experiments with different long-range delays and using a deeper threshold in the contour plot. Each one of the spectra obtained in this series of experiments, will show different long-range correlations, according to the value of  $^nJ(\text{C,H})$ . Actually, different delay times will enhance the proper signals and the rest may not be detected. This technique, optimized for small couplings, was employed to observe two and four-bond  $^1\text{H}$ - $^{13}\text{C}$  correlations and unambiguously assign the  $^{13}\text{C}$  NMR signals of several

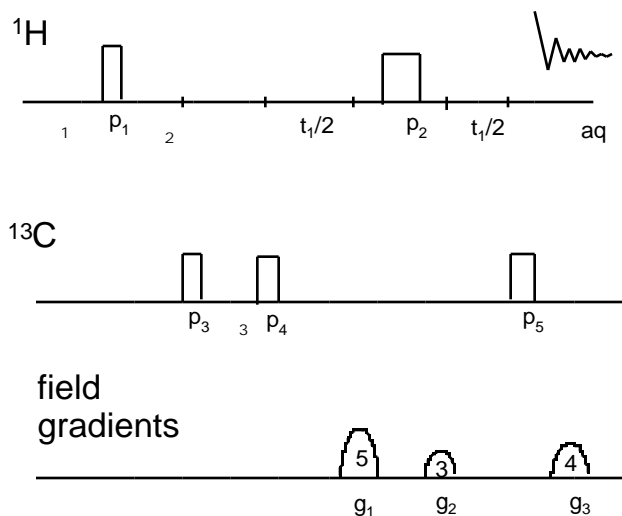


Fig. (1). Pulse sequence of the HMBC experiment.

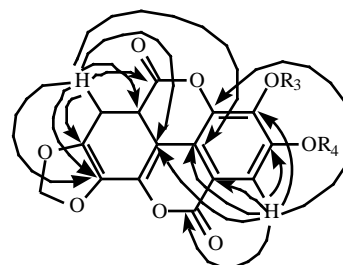
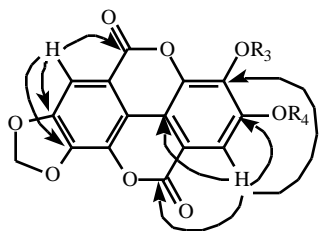
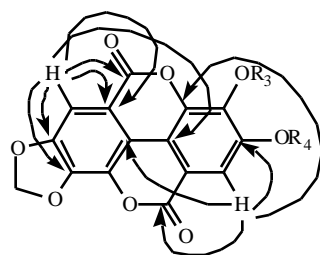


Fig. (2). Key HMBC correlations for ellagic acid derivative ( $\tau_2=50\text{ms}$ ,  $^nJ(\text{CH}) = 10\text{Hz}$ ).



**Fig. (3).** Key HMBC correlations for ellagic acid derivative ( $\tau=200\text{ms}$ ,  ${}^nJ(\text{CH}) = 2.5\text{Hz}$ ).

ellagic acid derivatives and related phenolic compounds, with highly oxygenated quaternary carbons [16]. These compounds contain several non-protonated aromatic carbons, and the assignment of these peaks, with close chemical shifts, is a significant challenge. The delay time,  $\tau=200\text{ms}$ , corresponding to a  ${}^nJ(\text{C,H})$  coupling of 2.5 Hz, is a compromise value which can increase the intensity of small coupling correlations, such as  ${}^4J(\text{C,H})$  and  ${}^2J(\text{C,H})$ , in the aromatic rings of phenolic compounds. Figs. (2), (3) and (4) show the correlations obtained with different  $\tau$  delay times.



**Fig. (4).** Key HMBC correlations for ellagic acid derivative ( $\tau=400\text{ms}$ ,  ${}^nJ(\text{CH}) = 1.25\text{ Hz}$ ).

The tricyclic quinone 4,4-dimethylanthracene-1,9,10(4H)-trione and eight derivatives with different substituents in the aromatic ring, Fig. (5), constitute another example of the use of long range correlations in spectral assignment. Here, the observation of an uncommon  ${}^5J(\text{CH})$  correlation, Table (1), was essential for the total assignment of the  ${}^{13}\text{C}$  spectra of some of these molecules. The observation of these long-range correlations,  ${}^5J(\text{CH})$  and  ${}^4J(\text{CH})$ , also depends on the pattern and nature of the substituents [17, 18]. The HMBC experiment was performed at 300 MHz ( ${}^1\text{H}$ ) and 75.47 MHz ( ${}^{13}\text{C}$ ), with  $\tau = 65\text{ms}$ . In this case, the modification of  $\tau$  from 65 ms ( ${}^nJ(\text{CH}) = 7.7\text{ Hz}$ ) to 100ms ( ${}^nJ(\text{CH}) = 5\text{ Hz}$ ) was not sufficient to show any differences in the observed correlations. This result suggests that in order to obtain longer range correlations in this family of compounds, the modification of  $\tau$  must be similar to the previous example.

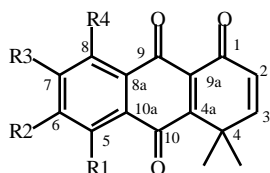


**Fig. (5).** 4,4-dimethylanthracene-1,9,10(4H)-trione derivatives.

## NEW PULSE SEQUENCES

In recent years there have been several attempts to improve the results of the HMBC experiment, mainly focused on the question of optimization of the  $\tau$  delay. In the decoupled HMBC (D-HMBC) [19] experiment, the first approach of Furihata and Seto was to introduce an additional delay time after the  ${}^{13}\text{C}$   $90^\circ$  X pulse, to refocus the  ${}^1\text{H}$  magnetization, and broad band proton decoupling for the  ${}^{13}\text{C}$  nucleus. As a result of these modifications, a fan-out of the  ${}^1\text{H}$  magnetization is prevented, giving in-phase signals with better signal to noise ratios. Under this condition the data are acquired in the phase sensitive mode by elimination of the signal/noise decreases due to poor digital resolution. D-HMBC also has been described to facilitate the observation of  ${}^{13}\text{C}$ - ${}^1\text{H}$  long-range correlations with small coupling constants.

The cross peaks observed in the D-HMBC experiment of promothiocin B, with a shorter delay time, also are observed when a longer delay is employed, Figs. (6) and (7). However, this correlation could not be observed in the standard HMBC spectra, even if the same delay time was employed, mainly due to poor signal to noise ratio.

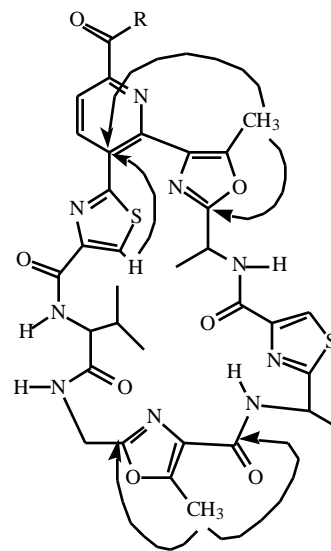


**Fig. (6).**  ${}^4J(\text{CH})$  and  ${}^5J(\text{CH})$  correlations observed in the D-HMBC spectra of promothiocin B. With  $\tau = 120\text{ ms}$ .

The same authors, after having described the D-HMBC experiment, published another paper introducing a 3D modification of this experiment, namely 3D-HMBC [20]. The basic idea was to acquire a series of HMBC spectra differing in the value of the long range delay. Therefore, successive planes in the 3D-HMBC experiment differ only in the long-range coupling for which they are optimized. In this fashion, a convenient technique is provided to sample a variety of potential C,H long-range correlations. The drawback of this experiment is the inconvenience of having to perform a series of 2D experiments, which may cause problems particularly in diluted samples.

More recently, the same authors have reported a couple of new experiments, CT-HMBC-1 and the improved version

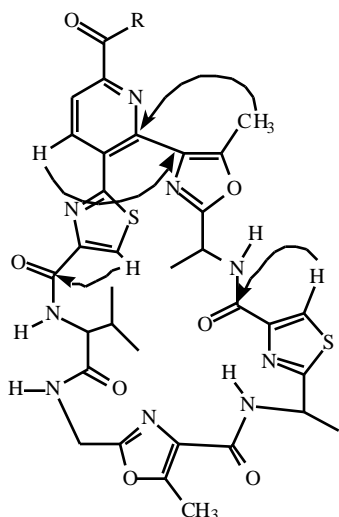


**Fig. (7).**  $^3J(\text{CH})$  and  $^4J(\text{CH})$  correlations observed in the D-HMBC spectra of promothiocin B. With  $t_2 = 500$  ms.

CT-HMBC-2. These experiments incorporate a pair of constant evolution times [21]. They employ a conventional “static” long-range delay optimization and then incorporate a decremented delay. The last pulse sequence suppresses the  $^1\text{H}$ - $^1\text{H}$  coupling modulation in  $F_1$ , as in the former, but also modulate the range of  $^1\text{H}$ - $^{13}\text{C}$  coupling in  $F_1$ , introducing the “variable” long-range transfer delay.

Perhaps the most important modification of the long-range heteronuclear shift correlation experiments was the ACCORD-HMBC experiment described by Wagner and Berger [22]. This technique uses the “accordion principle” [23] to sample a range of long-range heteronuclear coupling constants. Here the long-range delay used for the heteronuclear couplings systematically decreases, and the symmetry of the experiment is maintained, decreasing the refocusing delay after the last pulse and the acquisition. The

pulse sequence parameters are adjusted in such a way that values of the heteronuclear coupling constants between 2-25 Hz are sampled, with the smaller values of the variable delay at the initial  $t_1$  increments, and the higher values towards the end of the  $t_1$  evolution. To minimize phase distortions and frequency offsets in  $F_1$ , this process is repeated after the back transfer from carbons to protons, thus the  $180^\circ$  proton pulse is always exactly in the middle of the sequence. The final result is equivalent to observing a series of selected long-range correlations in a single experiment. Furthermore, the symmetrical nature of this technique permit heteronuclear decoupling to be applied during acquisition, increasing the signal to noise ratio. The ACCORD-HMBC experiment is one of the most interesting and convenient modifications of HMBC, since it allows a significantly wider range of long-range couplings to be sampled simultaneously in a single experiment. However, one of the inconveniences is the fact that the “accordion” variable delay acts as a third evolution time for  $F_1$   $^1\text{H}$ - $^1\text{H}$  frequency modulation of the long-range correlations to be observed.

Martin’s group has elaborated two pulse sequences to improve this behavior, named Improved Performance Accordion Heteronuclear Multiple-Bond Correlation Spectroscopy: IMPEACH-MBC [24], and Constant Time Inverse-Detection Gradient Accordion Rescaled Heteronuclear Multiple Bond Correlation: CIGAR-HMBC [25]. These two modifications improve the original version of the experiment and both methods offer the capability to sample broad ranges of potential long-range couplings in a single experiment. The IMPEACH-MBC experiment [24] incorporates a variable delay that decreases according to the expression  $(t_{\max} - t_{\min})/n_i$ , with  $n_i$  equal to the number of increments of the evolution time used to digitize the frequency domain, as the evolution periods  $t_{1/2}$  are incremented by  $t_1$ . This modification partially or completely suppresses  $^1\text{H}$ - $^1\text{H}$  coupling modulation, inherent to the utilization of the accordion principle, while it is still able to sample a significant range of potential long-range heteronuclear couplings. In effect,  $F_1$  homonuclear coupling modulation of

**Table 1.** Four and Five-bond Long-range Correlations for 4,4-Dimethylanthracene-1,9,10(4H)-trione Derivatives

compound	R <sub>1</sub>	R <sub>2</sub>	R <sub>3</sub>	R <sub>4</sub>	$^nJ(\text{CH})$	$^5J(\text{CH})$
1	H	H	H	H	C-10 to H-3	C-10a to H-3, C-9 to H-3
2	H	Me	Me	H	C-10 to H-3	--
3	Me	H	H	H	5-Me to C-10, C-10 to H-3	--
4	H	Me	H	H	--	--
5	H	H	Me	H	--	--
6	H	H	H	Me	8-Me to C-9, C-10 to H-3, C-10 to H-5	--
7	CH <sub>2</sub> OAc	H	H	Me	8-Me to C-9, CH <sub>2</sub> to C-10	C-9 to H-3
8	Me	H	H	CH <sub>2</sub> OAc	5-Me to C-10	C-9 to H-3
9	CH <sub>2</sub> OH	H	H	Me	--	--
10	CHO	H	H	Me	--	C-9 to H-3

long-range correlation can result in response overlap for highly congested spectral regions, or when limited digitization of the second frequency domain must be employed. In contrast, in IMPEACH-MBC experiment a constant time variable delay incorporated in the pulse sequence provides the means of suppressing  $F_1$  homonuclear coupling modulation, while still allowing broad ranges of potential long-range couplings to be sampled in a single experiment. The CIGAR-HMBC experiment [25] constitutes a further refinement of the IMPEACH-MBC. It modifies the constant time variable delay of the IMPEACH-MBC pulse sequence, to allow a user-determined scaling factor,  $J_{scale}$ , of  $F_1$  modulation to either decrease it to a minimum or remove it completely. This is achieved by modifying the incrementation of  $D/2$ , contained in the constant time variable delay pulse sequence element introduced in the IMPEACH-MBC experiment. It allows a better control of the  $F_1$  H-H modulation of the long-range correlations to be observed. According to the authors [25], the CIGAR-HMBC pulse sequence is probably the best available accordion type of experiment to be used in structure elucidation of complex organic molecules. This refinement allows the operator to reintroduce whatever degree of  $F_1$  modulation is desired to authenticate weak long-range responses. The performance of this experiment was compared with results obtained for identically optimized and processed ACCORD-HMBC and IMPEACH-MBC spectra of strychnine. Although qualitatively the responses were similar, the ACCORD-HMBC has fewer long-range responses from some of the protons than the spectra obtained with the other two experiments. However, there are some long-range responses detected in the ACCORD-HMBC spectrum which are not observed with either IMPEACH-MBC or CIGAR-HMBC, despite the identical optimization. Martin also has discussed the advantages of the accordion optimization [26]. Both experiments, IMPEACH-MBC and CIGAR-HMBC, provide much better experimental access to sample long-range couplings, which may be crucial in the structure elucidation of molecules which possess a relatively proton deficient skeleton.

In the next pages, a series of examples of observation of long-range  $^1\text{H}$ - $^{13}\text{C}$  correlations, using the HMBC experiment, to elucidate the structures of a variety of natural products, are given. In most cases the authors do not refer explicitly to the long range correlation delay used. Therefore, we will only mention it when the original authors have pointed it out. The most common correlations observed arise from two and three bond coupling constants; however, four bond correlations have also been observed. Five bond correlations are unusual and six bond correlations are very uncommon. The next figures show only correlations from four to six bonds, two and three bond correlations do not appear.

## HETEROCYCLES

One of the first papers reporting the observation of four-bond long-range coupling in an HMBC spectrum was the case of distamycin A. The observation of a  $^4J_{\text{CH}}$  couplings from the H-5 aromatic proton to the carbonyl, linking one pyrrole to the preceding pyrrole ring, was crucial for the

complete assignment of the distamycin A structure [27], see Fig. (8). This example was early cited in a review by Martin [5].

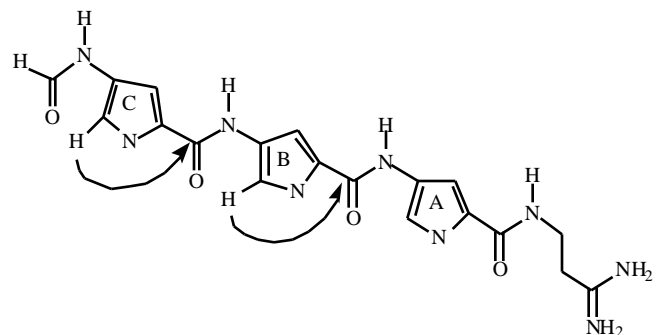


Fig. (8). Four-bond long-range correlations for distamycin A.

Two new pyridoacridine alkaloids were isolated from the ascidian *Cystodytes* sp., arnoamines A and B [28], see Fig. (9). Both of these structures possess a pyrrole ring fused to the pyridoacridine ring system. The HMBC spectra of arnoamine A and B show four-bond C,H correlations in addition to the usually observed three-bond correlations. The four-bond coupling constants seem to change markedly when the hydroxyl group is replaced by a methoxy group, enough to make some four-bond long-range correlation to appear and others become undetectable.

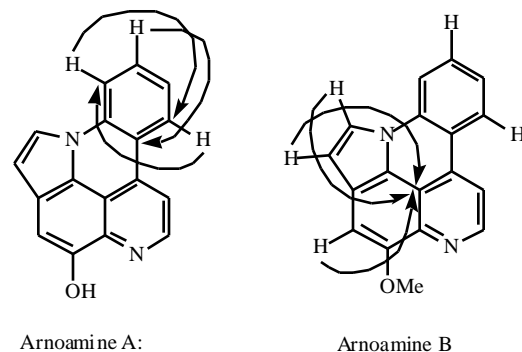


Fig. (9). Four-bond long-range correlations for arnoamines A and B.

The cytotoxic epymeric heterocycles asmarines A and B, a new class of nitrogen containing metabolites, were isolated from the marine sponge *Raspailia* sp. Their structures were elucidated using spectroscopic techniques. The HMBC spectra of both compounds show a four-bond long-range correlation through nitrogen atom [29]. Fig. (10).

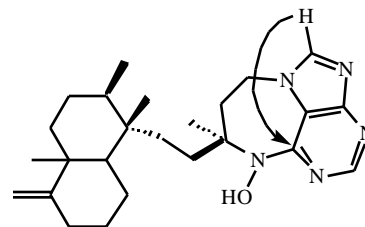


Fig. (10). Four-bond long-range correlation for asmarines A and B.

## MONOTERPENES

The monoterpene glycoside mudanpioside F, isolated from the root bark of *Paeonia suffruticosa* [30], displays an HMBC spectrum which exhibits a four-bond long-range C,H correlation between one of the methyl carbons and H-6. Fig. (11).

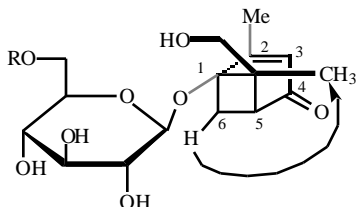


Fig. (11). Four-bond long-range correlation for mudanpioside F.

## DITERPENES

A spiro lactone diterpene of the clerodane type, heteroscypholide A, was isolated from the cells of a suspension culture of the liverwort *Heteroscyphus planus* [31]. It also shows two  $^4J(\text{CH})$  long-range correlations between the protons of a methyl group and a vinylic carbon across the double bond. The other correlation is from the carbon atom of a methyl group and a proton located on the same side of the molecule. This observation allowed the authors to join two structural fragments. Fig. (12).

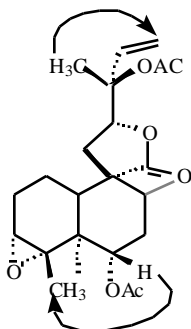


Fig. (12). Four-bond long-range correlations for heteroscypholide A.

## TRITERPENES

A new class of triterpenoids isolated from the roots of *Dichapetalum madagascariense*, dichapetalins has been reported [32]. One of them, dichapetalin D, shows a four-bond long-range correlation between the methyl group of an ester moiety and the carbon atom. Fig. (13).

22-Acetoxy-15-deoxy-eucosterol, a new spirocyclic nortriterpene, has been isolated from the bulbs of *Veltheimia viridifolia* [33]. The authors performed two experiments with the long-range delay optimized for two values of coupling: 10 and 7 Hz. In the experiment optimized for the 7 Hz coupling, C-12 showed a cross-peak only with the

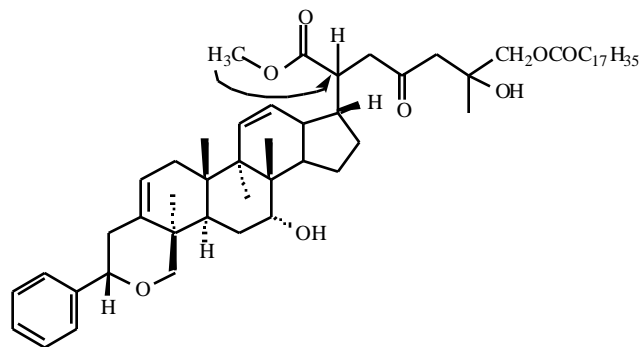


Fig. (13). Four-bond long-range correlations for dichapetalin D.

protons bonded to C-18, a methyl group, while in the experiment optimized for a 10 Hz coupling, a four-bond long-range correlation between C-12 and H-20 was observed. Fig. (14).

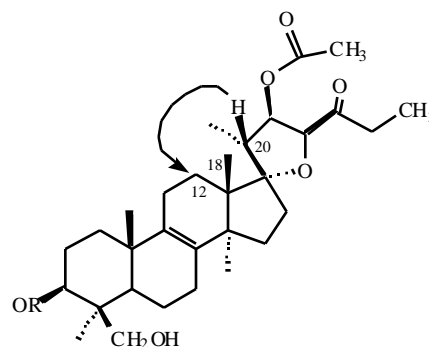


Fig. (14). Four-bond long-range correlation for 22-acetoxy-15-deoxy-eucosterol.

## SESQUITERPENES

1,2-Dehydro-3-oxo- -gurjunene (aromadendrane skeleton), obtained from *Calypogeia azurea*, shows several four-bond long-range correlations in a recently reported HMBC spectrum [34]. These are shown in Fig. (15).

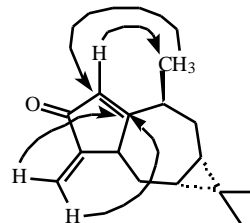
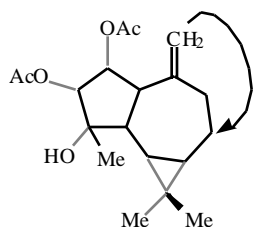


Fig. (15). Four-bond long-range correlations 1,2-dehydro-3-oxo- -gurjunene.

Another example of terpenoids that exhibit this kind of long-range heteronuclear correlations,  $^4J(\text{CH})$ , is planotriol diacetate, obtained from cultured cells of the liverwort *Heteroscyphus planus*, see Fig. (16). The structure of this compound corresponds to an *ent*-alloaromadendrane [35].



**Fig. (16).** Four-bond long-range correlation of planotriol diacetate.

## QUINONES

Three sesquiterpene *ortho*-naphthoquinones, davidianones A, B and C, isolated from *Ulmus davidiana*, show several four-bond long-range heteronuclear correlations, showing that the nature of the substituents in the aromatic ring can modify the pattern of long-range correlations in the same skeleton [36], Fig. (17).

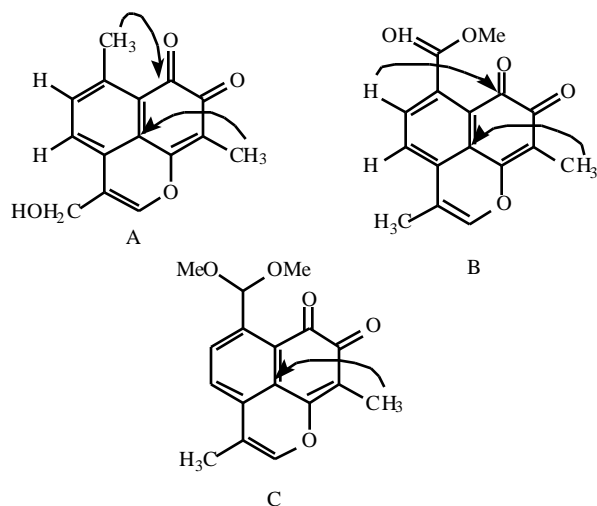


**Fig. (17).** Four-bond long-range correlations of davidianones A, B and C.

## ANTHRONES

Aloe barbendol (3,4-dihydro-3,5,7-trihydroxy-9-methyl-1(2H) anthracenone), isolated from *Aloe barbadensis*, shows a HMBC spectrum with two four bond long-range correlations, one from H-8 with the methyl carbon located at C-9, and the other one from the methyl protons with C-10a [37], Fig. (18).

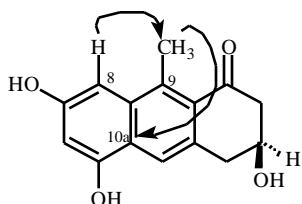


**Fig. (18).** Four-bond long-range correlations for Aloe barbendol.

## NAPHTALENONES

The binaphthalenone glycoside of Fig. (19), isolated from a methanol extract of the twigs of *Diospyros lycioides*, possesses antimicrobial activity. The HMBC spectrum, optimized for a  $J$  value of 8 Hz, shows two four-bond long-range correlations, which were used for the structural elucidation [38].

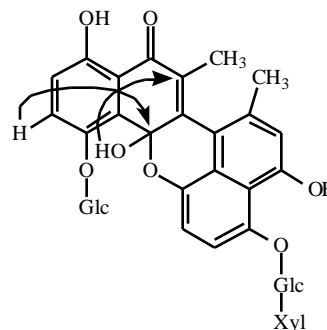


**Fig. (19).** Four-bond correlations for the binaphthalenone glycoside.

## NAPHTOPYRONES

Euplectin, a new naphthopyrone isolated from the lichen *Flavoparmelia euplecta*, shows two four-bond long-range correlations in the HMBC spectrum, which were particularly useful in the structure elucidation [39], Fig. (20)

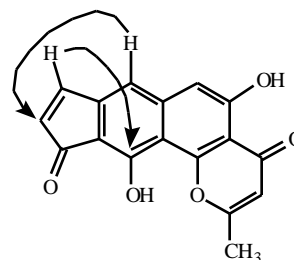


**Fig. (20).** Four-bond long-range correlations observed in the HMBC spectrum of euplectin.

## FLAVONOIDS

Licoagrocarpin, a new prenylated flavonoid isolated from the root cultures of *Glycyrriza glabra*, shows a correlation through four bonds in the HMBC spectrum [40], Fig. (21).

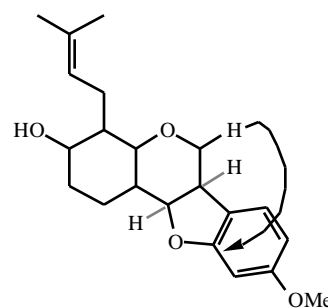


**Fig. (21).** Four-bond long-range correlation for licoagrocarpin.

The structure of patuletin, an acylated flavonol glycoside isolated from *Inula britannica*, was elucidated using HMBC. Fig. (22) shows the four-bond long-range correlation observed [41].

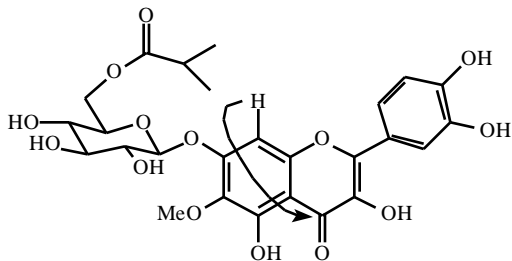


Fig. (22). Four-bond long-range correlation of patuletin.

### ACETYLENES

The four-bond correlations, shown in figure (23), were particularly helpful in the structure elucidation of petrocortyne E, a novel  $C_{46}$  polyacetylene isolated from a sponge of the genus *Petrosia*. This example serves to illustrate long-range correlation through triple bonds [42].

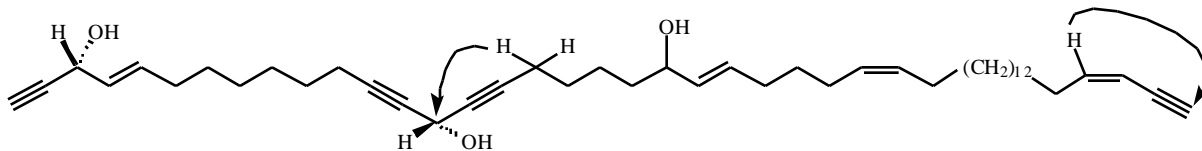


Fig. (23) . Four-bond long-range correlations correlations of petrocortyne E.

The HMBC spectrum of another polyacetylene, oropheic acid, obtained from the leaves of *Oropehea enneandra*, also shows a couple of four-bond long-range correlations through triple bond. Fig.(24) [43].

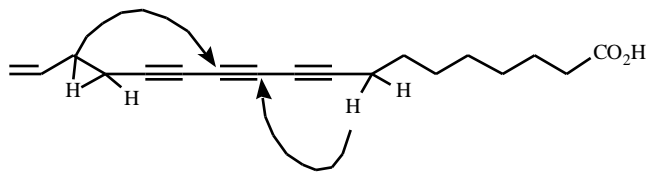


Fig. (24). Four-bond long-range correlations observed in oropheic acid.

Haliclonine, a polyacetylene carboxylic acid isolated from the marine sponge *Haliclona* sp. [44], also display a HMBC

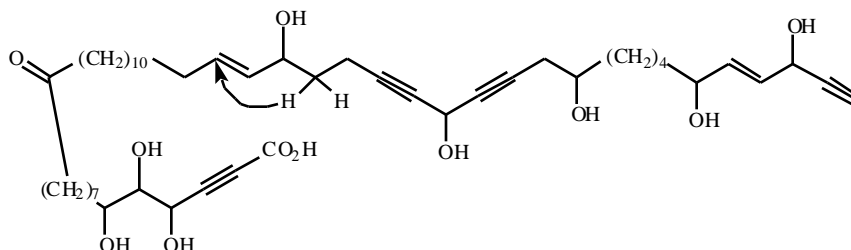


Fig. (25). Four-bond long-range correlations for haliclonine.

spectrum containing a four-bond long-range correlation. It was useful to assemble two molecular fragments. Fig. (25).

### CAROTENOIDS

The carotenoid glycoside ester of Fig. (26), was isolated from the thermophilic bacterium *Meiothermus ruber*. Its structure was determined with the aid of HMBC experiment and the four-bond long-range correlations through double bond and the glycosidic linkage were essential to determine its structure [45].

### STEROIDAL ALKALOIDS

The structure of the pregnane-type alkaloid, see Fig. (27), isolated from the roots and stems of *Sarcococca saligna*, was elucidated with the aid of HMBC. The HMBC spectrum of this compound exhibits two four-bond long-range correlations, one of them through the nitrogen atom of a saturated moiety of the molecule [46].

Trichoflectin, a bioactive azaphilone, was isolated from the ascomycete *Trichopezizella nidulus* [47], and its

structure was elucidated by spectroscopic methods, using the HMBC spectrum. It also shows a four-bond long-range correlation Fig. (28).

### HYDROXYLATED AROMATIC COMPOUNDS

The stilbene dimers, gnetuhainins A and E, were isolated from the lianas of *Gnetum hainanense* and their structures determined on the basis of chemical and spectral data [48]. The HMBC spectra of both gnetuhainins exhibit a four-bond long-range  $C,H$  correlation. Fig. (29).

Three novel complex C-glycosidic ellagitannins, named rhoipteleain H, I and J, were isolated from the fruits and bark of *Rhoiptelea chiliantha* [49]. The HMBC spectra of the rhoipteleain J was acquired using several long-range



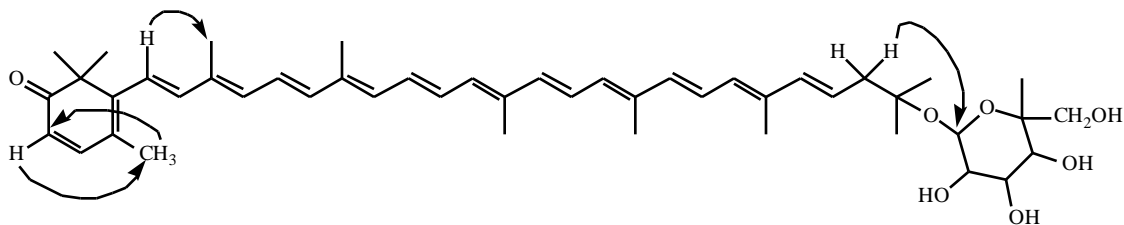


**Fig. (26).** Four-bond long-range correlations for carotenoid glycoside ester.

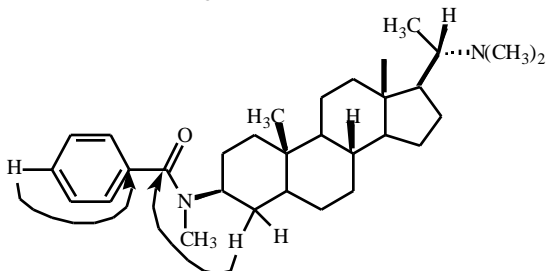


**Fig. (27).** Four-bond long-range correlations for pregnane-type steroidal alkaloid.

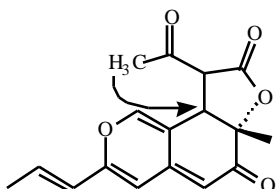


**Fig. (28).** Four-bond long-range correlations correlation for trichoflectin.

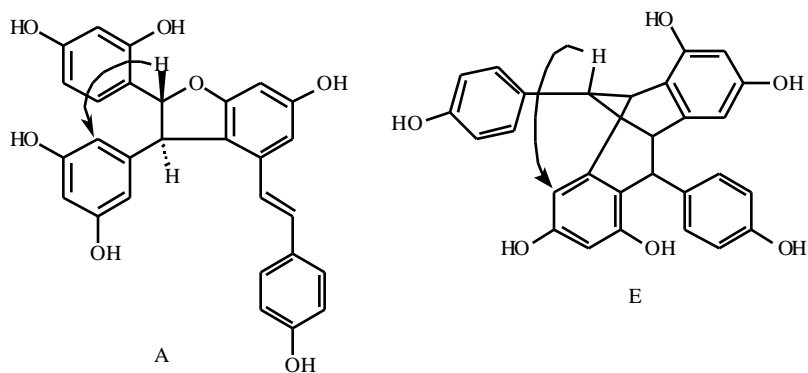


**Fig. (29).** Four-bond long-range correlations for gnetuhainins A and E.

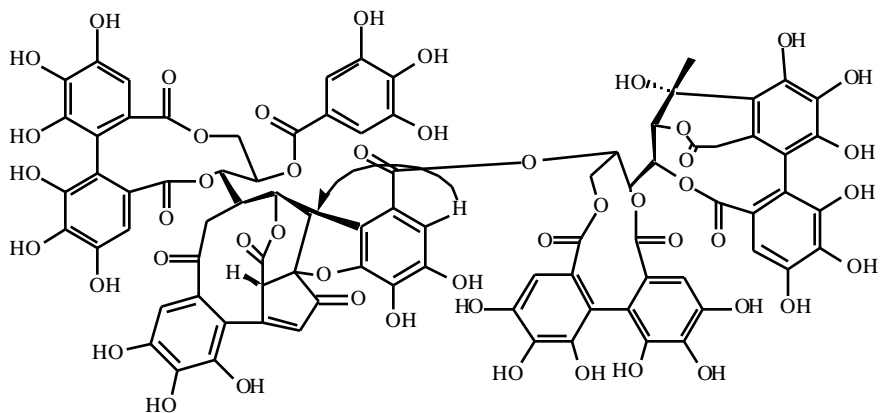


**Figure 30.** Four-bond long-range correlation for rhoipteanin J.

**Fig. (30).** Four-bond long-range correlation for rhoipteanin J.

delays. These were optimized for  ${}^1J_{CH} = 4, 6, 8, 10$  and  $12$  Hz. A four-bond long-range correlation is observed, but no

details about the long range delay used in this case was provided. Fig. (30).

Longithorols C, D and E, three new macrocyclic sesquiterpene hydroquinone metabolites, were isolated from the ascidian *Aplidium longithorax* [50]. The HMBC spectra were acquired using a log-range delay optimized for  ${}^nJ_{\text{CH}} = 8.3$  Hz, and showed the four-bond long-range correlations depicted in Fig. (31). This long-range correlation was of particular importance for the structure elucidation of longithorol E

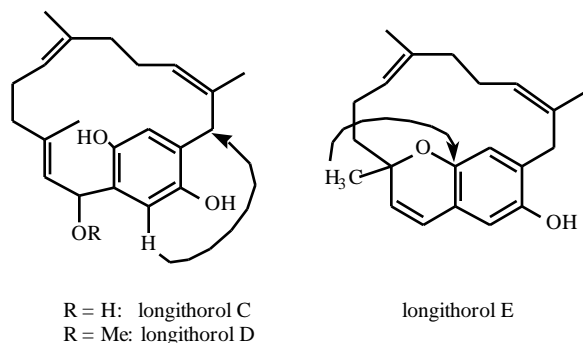


Fig. (31). Four-bond long-range correlations observed in the HMBC spectrum of longithorols.

The HMBC spectrum of oligostilbene malibatol B, isolated from the leaves of *Hopea malibato*, shows a four-bond long-range correlation. Fig (32) [51].

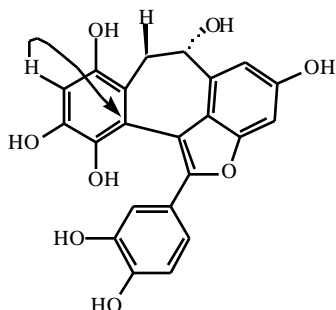


Fig. (32). Four-bond long-range correlation observed of malibatol B.

A new neolignan derivative isolated from *Onopordum illyricum* [52], showed two four-bond long-range correlations in the HMBC spectrum. One of them across a double bond of an aromatic system and the other one involves an aliphatic hydroxylic group across a saturated moiety. Fig. (33).

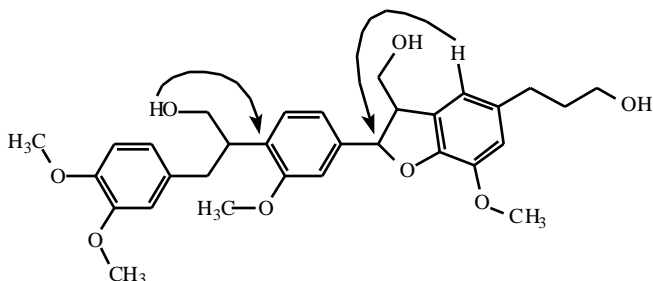


Fig. (33). Four-bond long-range correlations for neolignan derivative.

The HMBC spectrum of a new molokaiamine derivative, the wai'anaeamine B [53], a constituent of an *Verongid* sponge, shows a four-bond long-range correlation. Fig. 34.

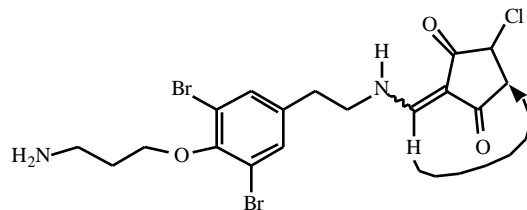


Fig. (34). Four-bond long-range correlation of wai'anaeamine B.

## SIX BONDS CORRELATIONS

27-O-cis,trans-*p*-coumaroylcylidiscic acid, obtained of aerial parts of *Kielmeyera coriacea* [54], shows a very long range correlation as shown in Fig. (35). Surprisingly the authors made no comments about this observation in the text, reporting this as a  ${}^6J(\text{CH})$  only through a figure, and give no experimental details about the long-range delay.

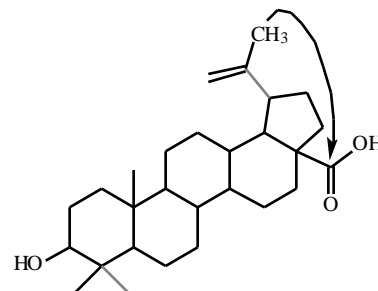


Fig. (35). Six-bond long-range correlation for 27-O-cis,trans-*p*-coumaroylcylidiscic acid.

## ACKNOWLEDGEMENT

The authors are pleased to acknowledge financial assistance from FONDECYT, Grant N° 1000859. W.C. and T.D-C. are grateful to DAAD and CONICYT, respectively, for their fellowships.

## REFERENCES

- [1] Bax, A.; Summers, M.F.; *J. Am. Chem. Soc.* **1986**, *108*, 2093.
- [2] Summers, M.F.; Marzilli, L.G.; Bax, A. *J. Am. Chem. Soc.* **1986**, *108*, 4285.
- [3] Bax, A.; Marion, D. *J. Magn. Reson.* **1988**, *78*, 186.
- [4] Martin, G.E.; Zektzer, A.S. Two Dimensional Methods for Establishing Molecular Connectivity. VCH, Weinheim **1988**.
- [5] Martin, G.E.; Crouch, R.C. *J. Nat. Prod.* **1991**, *54*, 1.

- [6] Martin, G.E.; Zektzer, A.Z. *Magn. Reson. Chem.* **1988**, *26*, 631.
- [7] Bax, A.; Subramanian, S; *J. Magn. Reson.* **1986**, *67*, 565.
- [8] Hurd, R.E.; Johr, B.K. *J. Magn. Reson.* **1991**, *91*, 648.
- [9] Ruiz-Cabello, J.; Vuister, G.W.; Moonen, C.T.W.; Van Gelderen, P.; Cohen, J.S. van Zijl, P.C.M. *J. Magn. Reson.* **1992**, *100*, 282.
- [10] Wilker, W.; Leibfritz, D.; Kerssebaum, R.; Bermel, W. *Magn. Reson. Chem.* **1993**, *31*, 287.
- [11] Braun, S.; Kalinowski, H.O.; Berger, S. *100 and More Basic NMR Experiments* p. 366. VCH, Weinheim **1996**.
- [12] Köck, M.; Reif, B.; Fenical, W.; Griesinger, C. *Tetrahedron Lett.*, **1996**, *37*, 363
- [13] Köck, M.; Junker, J.; Maier, W.; Will, M.; Lindel, T. *Eur. J. Org. Chem.* **1999**, 579.
- [14] Gasmi, G.; Massiot, G.; Nuzillard, J.M. *Magn. Reson. Chem.* **1996**, *34*, 185.
- [15] Reif, B.; Köck, M.; Kerssebaum, R.; Kang, H.; Fenical, W.; Griesinger, C. *J. Magn. Reson. Ser. A* **1996**, *118*, 282.
- [16] Li, X.-C.; Elsohly, H. N.; Hufford, C. D.; Clark, A. .M. *Magn. Reson. Chem.* **1999**, *37*, 856.
- [17] Araya-Maturana, R.; Cassels, B.K.; Delgado-Castro, T.; Hurtado-Guzmán, C. Jullian, C. *Magn. Reson. Chem.*, **1999**, *37*, 312.
- [18] Araya-Maturana, R.; Cardona, W.; Delgado-Castro, T.; Jullian, C. *Magn. Reson. Chem.*, **2000**, *38*, 135.
- [19] Furihata, K.; Seto, H. *Tetrahedron Lett.* **1995**, *36*, 2817.
- [20] Furihata, K.; Seto, H. *Tetrahedron Lett.* **1996**, *37*, 8901.
- [21] Furihata, K.; Seto, H. *Tetrahedron Lett.* **1998**, *39*, 7337.
- [22] Wagner, R.; Berger, S. *Magn. Reson. Chem.* **1998**, *36*, S44
- [23] Bodenhausen, G.; Ernst, R.R. *J. Am. Chem. Soc.* **1982**, *104*, 1304.
- [24] Hadden, C.E.; Martin, G.E.; Krishnamurthy, V.V. *J. Magn. Reson.* **1999**, *140*, 274.
- [25] Hadden, C.E.; Martin, G.E.; Krishnamurthy, V.V. *Magn. Reson. Chem.* **2000**, *38*, 143
- [26] Martin, G.E.; Hadden, C.E.; Crouch, R.C.; Krishnamurthy, V.V., *Magn. Reson. Chem.* **1999**, *37*, 517.
- [27] Williamson, D.S.; Smith, R.A.; Nagel, D.L.; Cohen S.M. *J. Magn. Reson.* **1989**, *82*, 605.
- [28] Plubrukarn, A.; Davidson, B.S. *J. Org. Chem.* **1998**, *63*, 1657.
- [29] Yosief, T.; Rudi, A.; Kashman, Y. *J. Nat. Prod.* **2000**, *63*, 299.
- [30] Lin, H.-C.; Ding, H.-Y.; Wu, T.-S.; Wu, P.-L. *Phytochemistry*, **1996**, *41*, 237.
- [31] Nabeta, K.; Oohata, T.; Ohkubo, S.; Sato, T.; Katoh, K. *Phytochemistry*, **1996**, *41*, 581.
- [32] Addae-Mensah, I.; Waibel, R.; Asunka, S. A.; Oppong, I. V.; Achenbach, H. *Phytochemistry*, **1996**, *41*, 649.
- [33] Amschler, G.; Frahm, A. W.; Müller-Doblies, D.; Müller-Doblies, U. *Phytochemistry*, **1998**, *47*, 429.
- [34] Tazaki, H.; Okihara, T.; Koshino, H.; Kobayashi, K. Nabeta, K. *Phytochemistry*, **1998**, *48*, 147.
- [35] Nabeta, K.; Ohkubo, S.; Hozumi, R.; Fukushi, Y. Nakai, H. Katoh, K. *Phytochemistry*, **1996**, *43*, 83]
- [36] Kim, J.-P.; Kim, W.-G.; Koshino, H.; Jung, J.; Yoo, I.-D. *Phytochemistry*, **1996**, *43*, 425.
- [37] Saleem, R.; Faizi, S.; Deeba, F.; Shaheen Siddiqui, B.; Husain Qazi, M. *Phytochemistry*, **1997**, *45*, 1279.
- [38] Li, X.-C.; Van der Bijl, P.; Wu, C.; *J. Nat. Prod.* **1998**, *61*, 817.
- [39] Ernst-Russell, M.A.; Chai, C. L.L.; Wardlaw, J. H. Elix, J. A. *J. Nat. Prod.* **2000**, *63*, 129.
- [40] Asada, Y.; Li, W.; Yoshikawa, T. *Phytochemistry*, **1998**, *47*, 389.
- [41] Jung Park, E.; Kim, Y.; Kim, J. *J. Nat. Prod.* **2000**, *63*, 34.
- [42] Shin, J.; Seo, Y.; Woong Cho, K.; *J. Nat. Prod.* **1998**, *61*, 1268.
- [43] Cavin, A.; Potterat, O; Wolfender, J.-L.; Hostettmann, K.; Dyatmyko, W. *J. Nat. Prod.* **1998**, *61*, 1497.
- [44] Chill, L.; Miroz, A.; Kashman, Y. *J. Nat. Prod.* **2000**, *63*, 523.
- [45] Burgess, M.L.; Barrow, K.D.; Gao, C. Heard, G. M.; Glenn, D. *J. Nat. Prod.* **1999**, *62*, 859.
- [46] Rahman, A.-U.; Anjum, S.; Farooq, A.; Riaz Khan, M.; Parveen, Z.; Iqbal Choudhary, M. *J. Nat. Prod.* **1998**, *61*, 202.
- [47] Thines, E.; Anke, H.; Sterner, O. *J. Nat. Prod.* **1998**, *61*, 306.
- [48] Huang, K.-S.; Wang, Y.-H.; Li, R.-L.; Lin, M. *J. Nat. Prod.* **2000**, *63*, 86.
- [49] Jiang, Z.-H.; Tanaka T.; Kouno, I. *J. Nat. Prod.* **1999**, *62*, 425.
- [50] Davis, R. A.; Carroll, A.R.; Quinn, R. J. *J. Nat. Prod.* **1999**, *62*, 1405.
- [51] Dai, J.-R.; Hallock, Y. F.; Cardellina II, J. H.; Boyd, M. R. *J. Nat. Prod.* **1998**, *61*, 351.
- [52] Braca, A.; De Tommasi, N.; Morelli, I.; Pizza, C. *J. Nat. Prod.* **1999**, *62*, 1371.
- [53] Lacy, C.; Scheuer, P.J. *J. Nat. Prod.* **2000**, *63*, 119.
- [54] García Cortez, D.A.; Young, M.C.M.; Marston, A. Wolfender, J.-L. Hostettmann, K. *Phytochemistry*, **1998**, *47*, 1367.